Supramolecular Chemistry
Publication details, including instructions for authors and subscription information:
http://www.informaworld.com/smpp/title~content=t713649759

Synthesis of a Series of *meso*-substituted Zinc Porphyrin Derivatives and their Assembly Dyad with Fulleropyrrolidine

Hua Xu[a]; Yi-Zhou Zhu[a]; Jian-Yu Zheng[a]
[a] State Key Laboratory and Institute of Elemento-Organic Chemistry, Nankai University, Tianjin, P. R. China

To cite this Article Xu, Hua , Zhu, Yi-Zhou and Zheng, Jian-Yu(2007) 'Synthesis of a Series of *meso*-substituted Zinc Porphyrin Derivatives and their Assembly Dyad with Fulleropyrrolidine', Supramolecular Chemistry, 19: 6, 365 — 376
To link to this Article: DOI: 10.1080/10610270600967046
URL: http://dx.doi.org/10.1080/10610270600967046

Supramolecular Chemistry, September 2007 Vol. 19 (6), pp. 365–372

Taylor & Francis
Taylor & Francis Group

Synthesis of a Series of *meso*-substituted Zinc Porphyrin Derivatives and their Assembly Dyad with Fulleropyrrolidine

HUA XU, YI-ZHOU ZHU and JIAN-YU ZHENG*

State Key Laboratory and Institute of Elemento-Organic Chemistry, Nankai University, Tianjin 300071, P. R. China

(Received 11 May 2006; Accepted 2 August 2006)

A series of *meso*-substituted zinc porphyrins (compounds 1–4) have been synthesized and their assembly dyads with [60]fullerene and fulleropyrrolidine compound (C_{60}-m, C_{60}-h) have been investigated. The stability of the assembly dyads are evaluated by UV–Vis and fluorescence titration methods and the result shows that the stability depends on the substituent groups in the porphyrin and fullerene moieties. Steady-state fluorescence spectroscopic studies of C_{60}-h assembly dyads with porphyrins 1–4 reveal efficient quenching between zinc porphyrin and C_{60}-h. Stable assembly dyad 4·C_{60}-h is constructed and efficient photoinduced electron transfer (PET) occurs between the zinc porphyrin and C_{60}-h moieties in this dyad.

Keywords: Porphyrin; Fullerene; Assembly; Multi-point binding; Photoinduced electron transfer

INTRODUCTION

Study of photoinduced energy and electron transfer (PET) in non-covalently linked synthetic arrays is very important to understand the processes that occur in the natural photosynthetic event [1–3]. In nature, the active components are rationally organized with suitable distance and orientation by a large number of weak, non-covalently interactions to optimize the rates of the processes. In recent years, due to their efficient PET and long-life charge separation state, porphyrin–fullerene assembly dyads with non-covalent bindings have been considered as one of the most important research targets [4–7]. Many self-assembly strategies including π–π interaction [8–13], axial coordination [14–19], hydrogen bonding [20,21] and crown ether-ammonium cation complexation formation [12,19] have been successfully applied to construct porphyrin–fullerene assemblies. Improved stability and efficient control over the distance and orientation are achieved by utilizing multi-point binding in a few instances. It is now well known that electron-transfer efficiency is sensitive to the stability of assembly dyads and distance between the donor and the acceptor. Thus, it occurs to us that the efficient electron-transfer in this dyad would be achieved by multi-point binding mode.

Although covalently linked multi-porphyrin has been successfully applied in designing multi-point binding strategy assemblies [8–11,13,18], the synthesis has been proved to be difficult, therefore, the considerable synthesis for further study is a very tough work, which imposed a limit on the application of porphyrin–fullerene assembly dyads. On the other hand, examples of assembly dyads constructed by monoporphyrin, which are similar to natural systems, are relatively few except those built through the axial coordination of the pyridyl moieties in fullerene with the metal ion of the porphyrins [14–17]. Other monoporphyirn–fullerene assembly dyads based on the second-generation dendritic substituents porphyrin are also reported, however, the synthesis is very difficult [22]. Therefore, it is important to construct a stable assembly dyad by facilely synthesized monoporphyrins and fullerene compound. So in this paper, we synthesize a series of *meso*-substituted monoporphyrins (**1**–**4**) and fulleropyrrolidine compounds (**C_{60}-m, C_{60}-h**) [23] (Scheme 1) and investigate the impact of different functional groups in porphyrin and fullerene

*Corresponding author. Tel.: + 86-22-2350-5572. Fax: + 86-22-2350-5572. E-mail: jyzheng@nankai.edu.cn

ISSN 1061-0278 print/ISSN 1029-0478 online © 2007 Taylor & Francis
DOI: 10.1080/10610270600967046

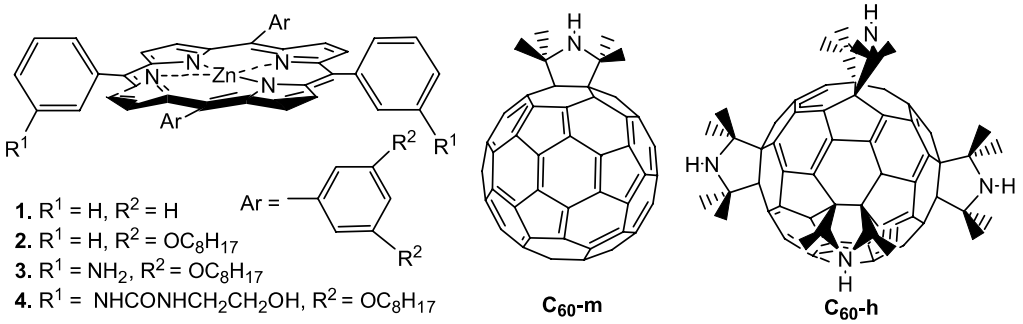

SCHEME 1 Porphyrins **1**–**4** and fulleropyrrolidine compound (**C_{60}-m**, **C_{60}-h**).

moieties on the stability of their assembly dyads. D_3-symmetry fullerene derivative (**C_{60}-h**) bears six pyrrolidines symmetrically distributing on the surface of fullerene sphere, and the α,α-atropisomer zinc porphyrins [24–28] are designed with substituted groups on one side of the porphyrin plane. The assembly dyads are supposed to be constructed through the multi-hydrogen bonds of pyrrolidines on fullerene moieties and hydroxylethyl ureas on porphyrins, together with the axial coordination of nitrogen atom of fulleropyrrolidine and zinc ion in porphyrin, to improve their stability and photo-induced electron transfer efficiency (Fig. 1).

RESULTS AND DISCUSSION

The synthetic approach of *meso*-substituted zinc porphyrins **2**–**4** is shown in Scheme 2. The synthesis was simplified owing to the symmetry of porphyrins **2**–**4** by classical [2+2] Lindsey methodology [29,30]. Dioctyloxy benzaldehyde **6** was synthesized by the alkylation of dihydroxybenzyl alcohol **5**, followed by oxidation with DDQ. Porphyrin **9a** or **9b** was prepared in yields of 15% and 18% respectively by trifluoroacetic acid-catalyzed reactions of **6** and **8a** or **8b**. The amino-functionalized porphyrin **10** was obtained by reduction of the nitro groups of **9a** with $SnCl_2{\cdot}2H_2O$ in acidic medium. Porphyrin **11** was obtained by reaction of **10** with triphosgene in dry dichloromethane containing a small amount of dry Et_3N, followed by treating the obtained isocyanate intermediate with ethanolamine [24–28,31]. After purification and separation by chromatography, α,α-bisaminoporphyrin **11** [32] was obtained in a overall yield of 34%. Metalations of porphyrins **9b**, **10** and **11** were accomplished almost quantitatively using a methanol saturated solution of zinc acetate to afford zinc porphyrins **2**–**4**. The four octyloxyl groups were introduced into *meso*-phenyl rings of the porphyrins **2**–**4** moieties to improve their hydrophobicity and solubility in organic solvents such as choloroform, dichloromethane and toluene. Structures of porphyrins **2**–**4** were identified by ^{1}H NMR, ^{13}C NMR, UV–Vis spectra, ESI-MS and HR-MS analysis.

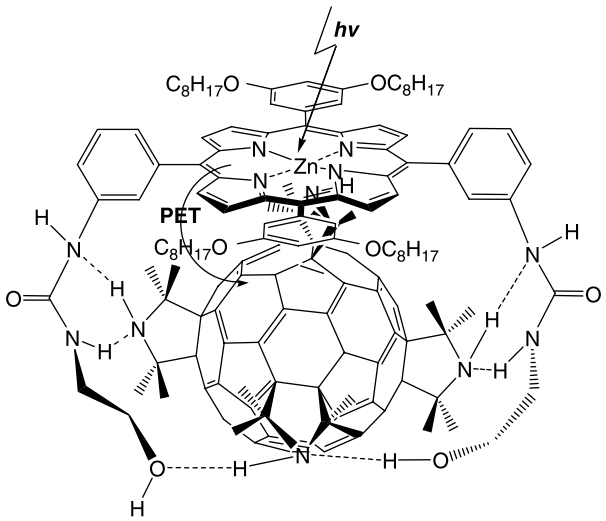

FIGURE 1 Self-assembly of **4·C_{60}-h** dyad through multi-point binding mode.

Stability of assembly dyads of porphyrins and fullerenes was first measured by UV–Vis titration method. When titration of **C_{60}-h** to the solutions of porphyrins **1**–**4** ($\sim 1.0 \times 10^{-6}$ M), only the spectra of **3** and **4** showed obvious hypochromic effect with red shift of the Soret bands absorption (from 427–429 nm and 422–423 nm), and an isosbestic point at 428 nm and 426 nm, respectively (Fig. 2). This spectral change is coincident with the recently reported results [8–21]. A Job's method of continuous variation plots confirmed a formation of 1:1 complex (see Appendix Fig. S1). The binding constants ($\mathbf{K_{abs}}$) [33] evaluated from the change in Soret absorbance are listed in Table I. The largest binding constant for **4·C_{60}-h** complex indicated that the binding of porphyrin **4** to **C_{60}-h** was more strongly than porphyrin **1**–**3**. This is ascribed that the introduction of suitable functional groups into porphyrin **4**, adopting a multiple bonding mode with **C_{60}-h**, enhances the stability of **4·C_{60}-h** dyad. The same results were observed both in toluene and dicholormethane solution. In addition, complex-induced chemical shift change in ^{1}H NMR spectra

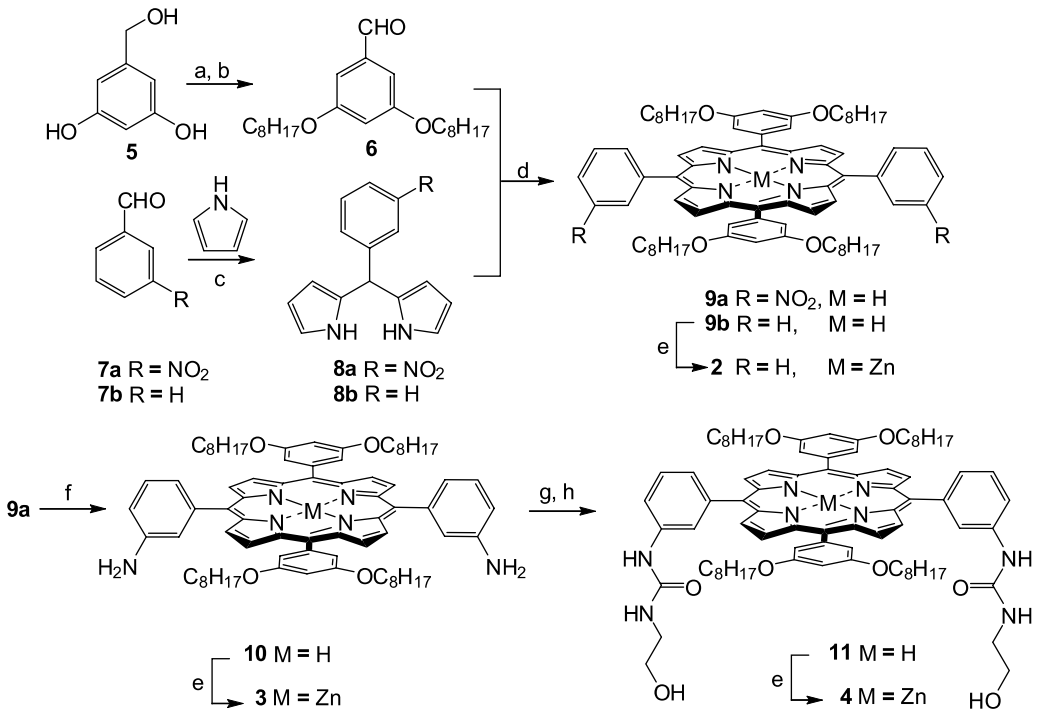

SCHEME 2 Synthesis of zinc porphyrins **2**–**4**. Reagents and conditions: (a) 1-bromooctane, K_2CO_3, DMF, 70–80°C, 72 h, 85%. (b) DDQ, CH_2Cl_2, r.t, 6 h, 87%. (c) TFA, r.t, 15 min, 72%. (d) TFA, DDQ, r.t, 18%. (e) $Zn(OAc)_2$, $CHCl_3$/MeOH, reflux, 6 h, 90%. (f) $SnCl_2{\cdot}2H_2O$, 65°C, 45 min, 70%. (g) Triphosgene, Et_3N, CH_2Cl_2, r.t, 2 h. (f) Ethanolamine, CH_2Cl_2, r.t, 2 h, 34%.

(see Appendix Fig. S8) is ascribed that the formation of hydrogen bonds between **C_{60}-h** and introduced side chain groups of porphyrin **4**. All of these results revealed that the highest binding constant of porphyrin **4** with **C_{60}-h** was owing to the introduction of suitable substituent groups.

In contrast to porphyrins **1**–**3**, porphyrin **4** also exhibited relatively strong binding ability with fullerene (C_{60}) and mono-substituted fullerene compound (**C_{60}-m**) (Table I). This result can be ascribed that when more suitable functional groups are introduced into porphyrin **4**, its incorporating ability with C_{60} or **C_{60}-m** will be improved. The assembly dyad stability of porphyrin **4** and fullerene compounds decreased as reduction of the number of fullerene functional groups: **C_{60}-h** > **C_{60}-m** > C_{60} (Table I), which suggested that the degree of fullerene substitute also influenced the stability of assembly dyads.

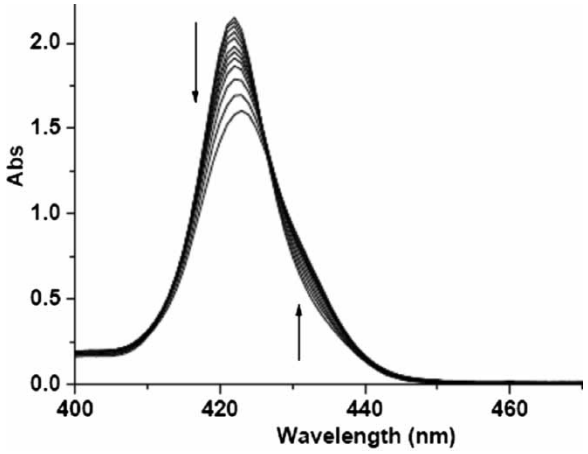

FIGURE 2 UV–Vis spectral changes of Soret band observed during the titration of **4** (1.09×10^{-6} M) with **C_{60}-h** (0–5.16×10^{-5} M) in toluene at 25°C. (the absorbance of **C_{60}-h** had been subtracted from the spectra).

In study of steady-state fluorescence of **4**, fluorescence quenching was observed with titration of **C_{60}-h**. As shown in Fig. 3a, upon increasing the **C_{60}-h** concentration in a toluene solution of porphyrin **4**, the fluorescence intensity of porphyrin **4** was obviously decreased, which supported a stable assembly dyad formation between porphyrin **4** and **C_{60}-h** along with the results of UV–Vis titration. In addition, it should be noticed that the fluorescence intensity increased at 500–600 nm and simultaneously an isoemissive point appeared at 598 nm (Fig. 3a). This could be either due to the occurrence of energy tranfer from porphyrin **4** or due to the direct excitation of **C_{60}-h** at the excitation wavelength of **4**. Blank control experiment of exiting **C_{60}-h** at 426 nm, a broad emission spectrum between 470 nm and 700 nm was observed, which indicated the direct excitation of **C_{60}-h** at the excitation wavelength of porphyrin **4** is possible. The emission of porphyrin **4** at the long wavelengths (562 nm) was also recorded with titration of **C_{60}-h**. In addition to a decrease of porphyrin **4** emission, **C_{60}-h** did not show obvious emission (Fig. 3b). This result clearly confirmed that

TABLE I Binding constants determined by UV–Vis ($K_{abs}/10^4\,M^{-1}$) and Fluorescence ($K_{em}/10^4\,M^{-1}$) titration spectra in toluene at 25°C

Comp.	K_{abs}	K_{em}	Comp.	K_{abs}	K_{em}
1·C_{60}	ND	ND	**2**·C_{60}	ND	ND
1·C_{60}-**m**	ND	ND	**2**·C_{60}-**m**	ND	0.23 ± 0.20
1·C_{60}-**h**	ND	0.65 ± 0.09	**2**·C_{60}-**h**	ND	0.63 ± 0.05
1·C_{60}-**h***	ND	0.73 ± 0.10	**2**·C_{60}-**h***	ND	0.65 ± 0.03
3·C_{60}	ND	ND	**4**·C_{60}	0.27 ± 0.02	0.16 ± 0.07
3·C_{60}-**m**	ND	0.26 ± 0.16	**4**·C_{60}-**m**	0.30 ± 0.02	0.26 ± 0.04
3·C_{60}-**h**	0.31 ± 0.02	1.14 ± 0.06	**4**·C_{60}-**h**	1.71 ± 0.20	1.74 ± 0.06
3·C_{60}-**h***	0.39 ± 0.05	0.93 ± 0.11	**4**·C_{60}-**h***	1.36 ± 0.48	1.55 ± 0.67

ND: no spectra variety detected;* in CH_2Cl_2.

the fluorescence observed of C_{60}-**h** really originated from direct excitation of C_{60}-**h** and not from energy tranfer of porphyrin **4**.

The fluorescence of porphyrins **1**–**3** were also quenched in the same way by C_{60}-**h**. The stability of assembly dyads of porphyrins **1**–**4** and C_{60}-**h** was in an order of **4** > **3** > **2** > **1**, in toluene and dicholoromethane (Table I). In contrast to porphyrin **1**, porphyrin **2** exhibited relatively high binding constant with C_{60}-**h**, which was ascribed to the increased hydrophobic interaction between C_{60}-**h** and porphyrin **2** through the introduction of four octyloxy groups. As for porphyrin **3**, introduction of amino groups would increase hydrogen bonding interaction, which further enhanced the stability of **3**·C_{60}-**h** assembly dyad. Introduction of more polar functional groups into porphyrin **4**, would form multiple bonding interactions, which resulted in the most stable **4**·C_{60}-**h** dyad. All the results obtained here suggested that the change of functional groups in porphyrin would strongly influence the stability of assembly dyad. Similar trends were also observed in cases of C_{60} and C_{60}-**m**.

As for fulleropyrrolidine compound, C_{60}-**h** exhibited much more strong fluorescence quenching ability than C_{60}-**m** and C_{60}, which was consistent with the results of UV–Vis titration (Table I). The increase in magnitude of the binding constant leads to the increase in fluorescence quenching efficiency and the binding constant K_{em} obtained from the fluorescence spectra changes validly corresponds to K_{abs}.

The observed fluorescence quenching indicates that there is a strong interaction between the excited state of porphyrin and fulleropyrrolidine compound. Possible pathway for the deactivation of excited porphyrin may be attributed to two competitive processes, energy transfer (ET) and photoinduced electron transfer (PET). In order to study the pathway of fluorescence quenching between porphyrin and fulleropyrrolidine moieties, the fluorescence quantum yield [34–36] of **4** and **4**·C_{60}-**h** dyad was investigated in solvents of different polarity and summarized in Table II. The fluorescence quantum yield of **4**·C_{60}-**h** dyad were obtained by mixture equal molar C_{60}-**h** with **4**. The significant decrease of the fluorescence quantum yield of **4**·C_{60}-**h** dyad was observed in contrast to that of **4**, in spite of the fluorescence quantum yield of **4** increased with increasing solvent's molecular dipole moment [37]. The fluorescence quenching percentage (Q) [38] in solvents of different polarity was estimated according

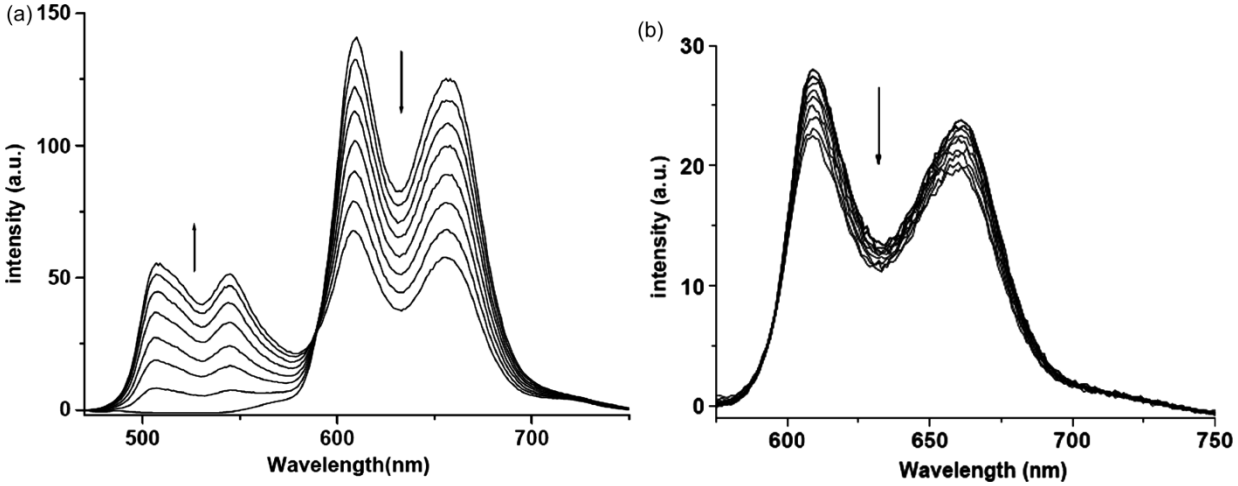

FIGURE 3 Fluorescence spectral changes observed during the titration of **4** (2.16×10^{-5} M) with C_{60}-**h** (0–1.6×10^{-4} M) in toluene at 25°C: (a) $\lambda_{ex} = 426$ nm (left); (b) $\lambda_{ex} = 562$ nm (right).

TABLE II Fluorescence quantum yields (Φ_f) and quenching percentage (Q) of porphyrin **4** and **4**·C_{60}—**h** assembly dyad in solvents of different polarity

Comp.	Solvent	Molecular Dipole Moment [34]	Φ_f[†]	Q(%)[‡]
4	Toluene	0.31	0.032	–
	CH_2Cl_2	1.14	0.033	–
	THF	1.75	0.036	–
4·C_{60}-**h**	Toluene	0.31	0.031	2.2
	CH_2Cl_2	1.14	0.031	6.7
	THF	1.75	0.032	11

[†] Measured at 298 K with reference to that of ZnTPP (in benzene, $\Phi_f = 0.033$). Solutions were deoxygenated by purging with N_2 before quantum yields were determined. The quantum yields have been corrected for the difference in solvent refractive index relative to that of benzene [34–36]. [‡] Quench of **4**·C_{60}-**h** relative to **4**.

to Eq. (1):

$$Q = \left(1 - \Phi_f^{P-F}/\Phi_f^{P}\right) \times 100\% \quad (1)$$

where Φ_f^{P-F} and Φ_f^{P} are the fluorescence quantum yield of **4**·C_{60}-**h** dyad and **4** respectively. The significant increase of the fluorescence quenching percentage of **4**·C_{60}-**h** dyad with increasing the solvent's molecular dipole moment (Table II) indicates that the quenching process in **4**·C_{60}-**h** dyad is dominated by the excited state electron transfer, as the energy transfer commonly does not depend on solvent polarity while the electron transfer tends to be sensitive to medium effects [39–43].

Kuciauskas *et al*. [44] have reported on some Zn porphyrin–fullerene dyads, showing that in apolar toluene medium, electron transfer prevail when the two moieties face to each other in close contact, whereas energy transfer occurs at longer intercomponent distances. Accordingly, since direct facing of the two chormophores in our case, the quenching mechanism tends to photoinduced electron transfer (PET). The detailed interaction mechanism is in process of research and will be reported in the future.

CONCLUSION

In conclusion, a series of novel porphyrin-fullerene non-covalent assembly dyads were designed and constructed, the stability of which could be enhanced by facilely variation of the functional groups in porphyrin and fullerene moieties. The assembly dyads can exist in either toluene or dicholormethane solution and can be investigated with common spectroscopic methods (UV–Vis, Fluorescence). The binding constants evaluated from the UV–Vis and fluorescence spectra indicate that the stability of assembly dyads lies on the introduction of suitable functional groups. Stable self-assembly dyad **4**·C_{60}-**h** was obtained and facilitated the effective electron transfer interactions between the excited zinc porphyrin and fullerene in this dyad. The present study provides a useful means of constructing stable functional supramolecular structures and illustrates the stability of non-covalent ensembles can be enhanced through introduction of suitable functional groups on constituent donor–acceptor pairs.

EXPERIMENTAL

General

The UV–Vis spectral measurements were measured on a Cary 300 UV–Vis spectrophotometer. The fluorescence emission were recorded on a Cary Eclipse fluorescence spectrophotometer. The ^{1}H NMR spectra studies were performed on a Bruker AV300 spectrometer. Chemical shifts (δ) are expressed in parts per million (ppm) using residual solvent protons as internal standards (chloroform: δ 7.26 ppm; DMSO: δ 2.49 ppm). The mass spectral analysis and high-resolution mass spectral (HR-MS) analysis were obtained on the Thermo Finnigan LCQ Advantage mass spectrometer and Bruker Deltonios FT-ICRMS.

Materials

Starting materials were commercially available unless noted otherwise. *meso*-tetraphenyl zinc porphyrin **1** was prepared according to literature procedures [45].

3,5-Bisoctyloxyphenyl Methanol

A mixture of K_2CO_3 (83 g, 0.6 mol), 3,5-dihydroxybenzyl alcohol (21 g, 0.15 mol) and 1-bromooctane (58 g, 0.3 mol) in anhydrous DMF (300 mL) was heated at 70–80°C for 72 h. After being cooled to room temperature, the mixture was filtered through a celite plate, and the filtration was concentrated under vacuum. The residue was mixed with ether, and the organic solution was washed with brine, dried over anhydrous $MgSO_4$, filtered and concentrated. The crude product was purified by column chromatography on silica gel (CH_2Cl_2). Yield 46.4 g (yield = 85%, colorless oil). ^{1}H NMR (300 MHz, $CDCl_3$): δ 6.49 (s, 2H, Phenyl-H), 6.37 (s, 1H, Phenyl-H), 4.61 (d, $J = 2.7$ Hz, 2H, —CH_2), 3.93 (t, $J = 6.6$ Hz,

4H, —OCH_2), 1.65–1.81 (m, 4H, —CH_2), 1.44–1.29 (m, 20H, —CH_2), 0.83–0.89 (m, 6H, —CH_3).

3,5-Dioctyloxy Benzaldehyde (6)

DDQ (11 g, 48.5 mmol) was added to a solution of 3,5-bisoctyloxyphenyl methanol (17 g, 46.7 mmol) in dioxane (200 mL). The reaction mixture immediately turned deep green (exothermic reaction), and $DDQH_2$ started precipitating within 1 min. TLC analysis indicated consumption of started material after 6 h. Filtered, the solvent was removed by vacuum evaporation. Treatment of the residue with dichloromethane left $DDQH_2$ undissolved. Filtered, evaporated, the residue was purified by column chromatography (CH_2Cl_2/PE; then Al_2O_3, CH_2Cl_2). Yield 14.7 g (y = 87%, colorless viscous oil solidified by refrigeration). ^{1}H NMR (300 MHz, $CDCl_3$): δ 9.86 (d, J = 2.1 Hz, 1H, —CHO), 6.96 (t, J = 2.1 Hz, 2H, Phenyl-H), 6.68 (q, J = 3.9 Hz, 1H, Phenyl-H), 3.94–3.99 (m, 4H, —OCH_2), 1.43–1.47 (m, 4H, —CH_2), 1.29–1.31 (m, 20H, —CH_2), 0.85–0.91 (m, 6H, —CH_3).

5-(3-Nitrophenyl)dipyrromethane (8a)

A mixture of pyrrole (120.84 g, 1.8 mol) and **6** (10.87 g, 72 mmol) was deoxygenated by bubbling N_2 through it for 15 minutes, then TFA was added and the mixture was stirred under N_2 for 15 minutes at ambient temperature. The reaction was quenched with 0.1 M NaOH aqueous solution and extracted with chloroform and washed with water. The excess pyrrole was removed under reduced pressure with slight heating and the residue was dissolved in minimal ethyl acetate and purified on a flash chromatography column (silica gel 200–300) using ethyl acetate and petroleum ether (1:10) as eluent. Yield 14.3 g (y = 72%, bright yellow solid). ^{1}H NMR (300 MHz, $CDCl_3$): δ 8.10–8.14 (m, 2H, pyrrole-H), 8.01 (br s, 2H, pyrrole-NH), 7.46–7.57 (m, 2H, pyrrole-H), 6.76 (s, 2H, phyenyl-H), 6.18 (d, J = 3 Hz, 2H, phyenyl-H), 5.90 (s, 2H, phyenyl-H), 5.59 (s, 1H, —CH—).

5,15-Bis(3,5-dioctyloxyphenyl)-10,20-bisphenylporphyrin (9b)

To a chloroform solution (300 mL) of a mixture of **8b** (0.445 g, 2 mmol) and **6** (0.724 g, 2 mmol) was added TFA (0.125 g, 1.25 mmol), and the mixture was stirred under argon for 2 h at room temperature. DDQ (0.908 g, 4 mmol) was added to the reaction mixture which was then stirred for 2 h at room temperature. The resulting mixture was subject to column chromatography on alumina. The solvent was removed by vacuum evaporation and the residue was chromatographed on silica gel column using $CHCl_3$/PE as eluent. Yield 150 mg (y = 15%, purple solid). ^{1}H NMR (300 MHz, $CDCl_3$): δ 8.96 (d, J = 4.8 Hz, 4H, pyrrole-H), 8.82–8.84 (m, 4H, pyrrole-H), 8.19–8.22 (m, 4H, phenyl-H), 7.73–7.78 (m, 6H, phenyl-H), 7.38 (d, J = 2.1 Hz, 4H, phenyl-H), 6.88–6.89 (m, 2H, phenyl-H), 4.11 (t, J = 6.6 Hz, 8H, OCH_2), 1.81–1.90 (m, 8H, CH_2), 1.26–1.53 (m, 40H, CH_2), 0.83–0.87 (m, 12H, CH_3), -2.81 (s, 2H, pyrrole-NH); UV-Vis: λ_{max}/nm 420, 515, 550, 589, 645; MS (ESI): m/z = 1127.80 (cal $C_{76}H_{95}N_4O_4^+$: 1127.73).

Zinc Porphyrin (2)

To a chloroform solution of **9b** (100 mg, 0.07 mmol), the methanol saturated solution of $Zn(OAc)_2{\cdot}2H_2O$ (200 mg, 1.48 mmol) was added and refluxed for 6 h, and the reaction mixture washed with water, dried over Na_2CO_3, and evaporated to dryness. The residue was subjected to column chromatography on silica gel with $CHCl_3$/PE as eluent. Yield 80 mg (y = 91%, purple solid). ^{1}H NMR (300 MHz, $CDCl_3$): δ 9.05–9.07 (m, 4H, pyrrole-H), 8.93 (d, J = 4.5 Hz, 4H, pyrrole-H), 8.20–8.22 (m, 4H, phenyl-H), 7.75 (d, J = 6.6 Hz, 6H, phenyl-H), 7.38 (s, 4H, phenyl-H), 6.87 (s, 2H, phenyl-H), 4.10 (t, J = 6.6 Hz, 8H, OCH_2), 1.80–1.87 (m, 8H, CH_2), 1.30–1.25 (m, 40H, CH_2), 0.82–0.86 (m, 12H, CH_3); ^{13}C NMR (300 MHz, $CDCl_3$): δ 14.1, 22.6, 26.1, 29.2, 29.4, 31.8, 68.4, 101.2, 114.3, 121.1, 121.1, 126.5, 127.5, 131.9, 131.9, 132.1, 134.4, 142.9, 144.5, 150.0, 150.1, 150.1, 150.2, 150.3, 158.2; UV–Vis: λ_{max}/nm 424 (ε/$mol^{-1}\,L^{-1}\,cm^{-1}$: 459000), 550 (21900); MS (ESI): m/z = 1188.97 (M^+). HR-MS (MALDI-FT): m/z = 1188.6417 (cal $C_{76}H_{92}N_4O_4Zn_1^+$: 1188.6404).

5,15-Bis(3,5-dioctyloxyphenyl)-10,20-bis(*m*-aminophenyl)porphyrin (10)

The bisnitroporphyrin **9a** was prepared on the basis of the method described for **9b** as a dark purple solid. The crude porphyrin **9a** was dissolved in 200 mL acetone, followed $SnCl_2{\cdot}2H_2O$ and 150 mL concentrated hydrochloric acid was added. The green solution was stirred at room temperature for 45 minutes and then heated to 65°C for 2 h. After the solution was cooled in ice, potassium hydroxide was added to bring the pH of the suspension higher than 10. The brown-violet mixture was stirred with 200 mL of chloroform for 10 minutes, the organic layer was separated, and 50 mL chloroform was used to wash the aqueous layer. All chloroform extracts were combined and washed three times with equal volumes of water and dried over anhydrous sodium sulfate. After evaporation of chloroform, the residue was purified on a silica column using $CHCl_3$ as eluent. Yield 0.93 g (y = 18%, purple solid).^{1}H NMR (300 MHz, $CDCl_3$): δ 8.93 (dd, J = 17.1 Hz and 4.8 Hz, 8H, β-pyrrole-H), 7.61 (d, J = 6.9 Hz, 2H, phenyl-H), 7.48–7.54 (m, 4H, phenyl-H), 7.37 (d, J = 1.5 Hz, 4H, phenyl-H), 7.10 (q, J = 2.1 Hz, 2H, phenyl-H), 6.88 (t, J = 2.1 Hz, 2H, phenyl-H), 4.11 (q, J = 6.3 Hz, 8H,

—OCH_2—), 3.94 (s, 4H, —NH_2), 1.81–1.89 (m, 8H, —CH_2—), 1.47–1.51 (m, 8H, —CH_2—), 1.27–1.31 (m, 32H, —CH_2—), 0.83–0.88 (m, 12H, —CH_3), −2.84 (s, 2H, pyrrole—NH). UV–Vis: λ_{max}/nm 423, 517, 552, 590, 645; MS (ESI): $m/z = 1157.89$ (cal $C_{76}H_{97}N_6O_4^+$: 1156.75).

Zinc Porphyrin (3)

Metalation **10** with zinc acetate according to zinc porphyrin **2**. Yield: 89%. ^{1}H NMR (300 MHz, $CDCl_3$): δ 8.92 (d, $J = 4.8$ Hz, 4H, β-pyrrole-H), 8.63–8.63 (m, 4H, β-pyrrole-H), 7.46–7.55 (m, 4H, phenyl-H), 7.33–7.38 (m, 4H, phenyl-H), 7.19–7.21 (m, 2H, phenyl-H), 6.88 (t, $J = 2.1$ Hz, 4H, phenyl-H), 5.52 (br s, 4H, —NH_2), 4.03–4.23 (m, 8H, —OCH_2—), 1.83–1.88 (m, 8H, CH_2), 1.22–1.31 (m, 40H, —CH_2—), 0.80–0.81 (m, 12H, —CH_3); ^{13}C NMR (300 MHz, $CDCl_3$): δ 14.0, 23.0, 26.1, 29.1, 29.3, 31.7, 68.6, 101.1, 113.8, 114.6, 119.9, 120.5, 122.7, 126.3, 126.6, 131.5, 132.3, 143.4, 145.0, 149.8, 158.2; UV–Vis: λ_{max}/nm 427 (ε/mol^{-1} L^{-1} cm^{-1}: 563000), 551 (25000); MS (ESI): $m/z = 1219.54$ (M^+). HR-MS (MALDI-FT): $m/z = 1218.6642$ (cal $C_{76}H_{94}N_6O_4Zn_1^+$: 1218.6623).

α,α-5,15-Bis(*m*-hydroxyethyl Urea)-10,20-bis(3,5-dioctyloxy-phenyl)porphyrin (11)

In the presence of nitrogen, triphosgene (78 mg, 0.26 mmol) in 5 mL dry dichloromethane was slowly added to 20 mL dry dichloromethane solution of **10** (233 mg, 0.2 mmol) containing dry Et_3N (160 mg, 1.5 mmol). The reaction mixture was stirred for 2 h at room temperature after which ethanolamine (160 mg, 2.61 mmol) in dichloromethane was added and stirred continued for another 2 h. The solvent was removed by rotavap and the residue was chromatographed on silica gel column using methanol and chloroform (3/100) as eluent. Yield 120 mg (y = 34%, purple solid). ^{1}H NMR (300 MHz, DMSO): δ 8.96 (br s, 2H, —PhNHCO—), 8.90 (dd, $J = 17.1$ Hz and 4.8 Hz, 8H, β-pyrrole-H), 8.35 (d, $J = 8.4$ Hz, 2H, phenyl-H), 7.61–7.79 (m, 6H, phenyl-H), 7.33–7.37 (m, 4H, phenyl-H), 6.92 (s, 2H, —CONH—), 6.32 (t, $J = 5.1$ Hz, 2H, phenyl-H), 4.76 (t, $J = 5.1$ Hz, 2H, —OH), 4.13 (s, 8H, —OCH_2—), 3.44 (q, $J = 9.6$ Hz, 4H, —NCH_2—), 3.15 (q, $J = 9.6$ Hz, 4H, —CH_2O—), 1.74–1.78 (m, 8H, —CH_2—), 1.42–1.43 (m, 8H, —CH_2—), 1.22–1.26 (m, 32H, —CH_2—), 0.78–0.80 (m, 12H, —CH_3), -2.97 (s, 2H, pyrrole-NH). UV-Vis: λ_{max}/nm 422, 516, 551, 590, 645; MS (ESI): $m/z = 1331.92$ (cal $C_{82}H_{107}N_8O_8^+$: 1331.81).

Zinc Porphyrin (4)

Metalation **11** with zinc acetate according to zinc porphyrin **2**. Yield: 87%. ^{1}H NMR (300 MHz, DMSO): δ 9.29 (br s, 2H, —PhNHCO—), 8.83 (dd, $J = 15$ Hz and 4.5 Hz, 8H, β-pyrrole-H), 8.28 (d, $J = 7.2$ Hz, 2H, phenyl-H), 7.57–7.78 (m, 6H, phenyl-H), 7.27–7.32 (m, 4H, phenyl-H), 6.90 (s, 2H, phenyl-H), 6.52 (br s, 2H, —CONH—), 4.76 (s, 2H, —OH), 4.14 (t, $J = 5.4$ Hz, 8H, —OCH_2—), 3.42 (q, $J = 9.6$ Hz, 4H, —NCH_2—), 3.14 (q, $J = 9.6$ Hz, 4H, —CH_2O—), 1.74–1.81 (m, 8H, —CH_2—), 1.43–1.45 (m, 8H, —CH_2—), 1.24–1.29 (m, 32H, —CH_2—), 0.80–0.83 (m, 12H, —CH_3). ^{13}C NMR (300 MHz, DMSO): δ 13.9, 22.0, 25.5, 28.6, 28.7, 31.2, 60.2, 67.7, 99.5, 100.4, 114.4, 116.4, 120.0, 120.3, 123.7, 126.7, 127.4, 131.3, 131.5, 138.6, 138.7, 143.1, 144.6, 149.0, 149.0, 149.2, 155.4, 155.5, 157.7; UV–Vis: λ_{max}/nm 431 (ε/mol^{-1} L^{-1} cm^{-1}: 186000), 561 (6330), 602 (2110); MS (ESI): $m/z = 1392.72$ (M^+). HR-MS (MALDI-FT): $m/z = 1392.7264$ (cal $C_{82}H_{104}N_8O_8Zn_1^+$: 1392.7274).

Binding Studies

For UV–Vis absorption titration experiment, typically aliquots of a fixed solution of the fullerene guests in toluene or dicholormethane were added to a toluene or dicholormethane solution of the porphyrin receptors, and the mixture was subjected to the UV–Vis spectroscopy at 25°C. The spectrum was corrected with a dilution factor and background subtraction. The difference in absorbance (ΔA) of the porphyrin receptor in the presence of the guest and absence of the guest was recorded and the data were plotted against [G]. The association constant K_{abs} for the 1:1 complexes was derived by applying a nonlinear curve-fitting method using a program origin 6.5 based on the equation [33]: $\Delta A = \Delta A_\infty((1 + K_{abs}[G] + K_{abs}[por]) - ((1 + K_{abs}[G] + K_{abs}[por])^2 - 4K_{abs}^2[por][G])^{0.5})/(2K_{abs}[por])$, where $\Delta A = A - A_0$, $\Delta A_\infty = A_\infty - A_0$ (ΔA_∞ is ΔA at infinite [por]), [G] = [**C_{60}-h**], [**C_{60}-m**] or [**C_{60}**]. For fluorescence experiment, titrations were carried out by addition a fixed solution of the fullerene guests in toluene or dicholormethane to a toluene or dicholormethane solution of the porphyrin receptors, and the mixture was subjected to the fluorescence spectroscopy at 25°C. The spectrum was corrected with a dilution factor and the association constant K_{em} was evaluated by applying a nonlinear curve-fitting method using a program origin 6.5 based on the equation [46]: $F/F_0 = (1 + P^*K_{em}[G])/(1 + K_{em}[G])$, where F_0 and F is the fluorescence intensity of porphyrin in the absence and presence of fullerene guest, respectively, [G] = [**C_{60}-h**], [**C_{60}-m**] or [**C_{60}**], $P = \varepsilon_P(\lambda_{exc})(d\phi_P/d\lambda)_{\lambda em}\Delta\lambda/\varepsilon_{P-F}(\lambda_{exc})(d\phi_{P-F}/d\lambda)_{\lambda em}\Delta\lambda$, ε_P and ε_{P-F} are the corresponding molar absorption coefficients, with the excitation wavelength in parentheses.

Acknowledgements

We thank the Natural Science Foundation of China (grant 20172028 and 20421202) and the Trans-Century

Training Programme Foundation for the Talents by the State Education Commission (grant 2002—48) for their generous financial support.

References

[1] Wasielewski, M. R. *Chem. Rev.* **1992**, *92*, 435.
[2] Ward, M. D. *Chem. Soc. Rev.* **1997**, *26*, 365.
[3] Flamigni, L.; Johnston, M. R. *New J. Chem.* **2001**, *25*, 1368.
[4] Guldi, D. M. *Chem. Soc. Rev.* **2002**, *31*, 22.
[5] Satake, A.; Kobuke, Y. *Tetrahedron* **2005**, *61*, 13.
[6] Konishi, T.; Ikeda, A.; Shinkai, S. *Tetrahedron* **2005**, *61*, 4881.
[7] Boyd, P. D. W.; Reed, C. A. *Acc. Chem. Res.* **2005**, *38*, 235.
[8] Tashiro, K.; Aida, T.; Zheng, J. Y.; Kinbara, K.; Saigo, K.; Sakamoto, S.; Yamaguchi, K. *J. Am. Chem. Soc.* **1999**, *121*, 9477.
[9] Sun, D.; Tham, F. S.; Reed, C. A.; Chaker, L.; Burgess, M.; Boyd, P. D. W. *J. Am. Chem. Soc.* **2000**, *122*, 10704.
[10] Zheng, J. Y.; Tashiro, K.; Hirabayashi, Y.; Kinbara, K.; Saigo, K.; Aida, T.; Sakamoto, S.; Yamaguchi, K. *Angew. Chem., Int. Ed. Engl.* **2001**, *40*, 1858.
[11] Kubo, Y.; Sugasaki, A.; Ikeda, M.; Sugiyasu, K.; Sonoda, K.; Ikeda, A.; Takeuchi, M.; Shinkai, S. *Org. Lett.* **2002**, *4*, 925.
[12] Solladie, N.; Walther, M. E.; Gross, M.; Duarte, T. M. F.; Bourgogne, C.; Nierengarten, J. *Chem. Commun.* **2003**, 2412.
[13] Wu, Z. Q.; Shao, X. B.; Li, C.; Hou, J. L.; Wang, K.; Jiang, X. K.; Li, Z. T. *J. Am. Chem. Soc.* **2005**, *127*, 17460.
[14] Armarolin, N.; Diederich, F.; Echegoyen, L.; Habricher, T.; Flamignia, L.; Marconia, G.; Nierengarten, J. F. *New J. Chem.* **1999**, *23*, 77.
[15] D'Souza, F.; Deviprasad, G. R.; Rahman, M. S.; Chol, J. *Inorg. Chem.* **1999**, *38*, 2157.
[16] Wilson, S. R.; MacMahon, S.; Tat, F. T.; Jarowski, P. D.; Schuster, D. I. *Chem. Commun.* **2003**, 226.
[17] Tat, F. T.; Zhou, Z.; MacMahon, S.; Song, F.; Rheingold, A. L.; Echegoyen, L.; Schuster, D. I.; Wilson, S. R. *J. Org. Chem.* **2004**, *69*, 4602.
[18] D'Souza, F.; Gadde, S.; Zandler, M. E.; Itou, M.; Araki, Y.; Ito, O. *Chem. Commun.* **2004**, 2276.
[19] D'Souza, F.; Chitta, R.; Gadde, S.; Zandler, M. E.; Sandanayaka, A. S. D.; Araki, Y.; Ito, O. *Chem. Commun.* **2005**, 1279.
[20] Sessler, J. L.; Jayawickramarajah, J.; Gouloumis, A.; Torres, T.; Guldi, D. M.; Maldonadoa, S.; Stevenson, K. J. *Chem. Commun.* **2005**, 1892.
[21] D'Souza, F.; Deviprasad, G. R.; Zandler, M. E.; El-Khouly, M. E.; Fujitsuka, M.; Ito, O. *J. Phys. Chem.: A.* **2003**, *107*, 4801.
[22] Kimura, M.; Saito, Y.; Ohta, K.; Hanabusa, K.; Shirai, H.; Kobayashi, N. *J. Am. Chem. Soc.* **2002**, *124*, 5274.
[23] Schick, G.; Levitus, M.; Kvetko, L.; Johnson, B. A.; Lamparth, I.; Lunkwitz, R.; Ma, B.; Khan, S. I.; Garcia-Garibay, M. A.; Rubin, Y. *J. Am. Chem. Soc.* **1999**, *121*, 3246.
[24] Collman, P. J.; Fu, L. *Acc. Chem. Res.* **1999**, *32*, 455.
[25] Ruzie, C.; Michaudet, L.; Boitel, B. *Tetrahedron Lett.* **2002**, *43*, 7423.
[26] Collman, P. J.; Gagne, R. R.; Reed, C.; Halbert, T. R.; Lang, G.; Robinson, W. T. *J. Am. Chem. Soc.* **1975**, *97*, 1427.
[27] Wang, C. Z.; Zhu, Z. A.; Li, Y.; Chen, Y. T.; Wen, X.; Miao, F. M.; Chan, W. L.; Chan, A. S. C. *New J. Chem.* **2001**, *25*, 801.
[28] Lindsey, J. *J. Org. Chem.* **1980**, *45*, 5215.
[29] Arsenault, G. P.; Bullock, E.; MacDonald, S. F. *J. Am. Chem. Soc.* **1960**, *82*, 4384.
[30] Lee, C. H.; Lindsey, J. S. *Tetrahedron* **1994**, *50*, 11427.
[31] Collman, P. J.; Wang, Z.; Straumanis, A. *J. Org. Chem.* **1998**, *63*, 2424.
[32] The two atropisomer had no spectroscopic difference, but their R_f in TLC is a little different: αβ-atropisomer (4% $CH_3OH/CHCl_3$, $R_f = 0.7$), αα-atropisomer (4% $CH_3OH/CHCl_3$, $R_f = 0.6$); see ref [25,26]
[33] Guo, Y. M.; Oike, H.; Saeki, N.; Aida, T. *Angew. Chem., Int. Ed. Engl.* **2004**, *43*, 4915.
[34] Bolz, R. E.; Tuve, G. L. *CRC Handbook of Tables for Applied Engineering Science*; 2nd ed. CRC Press: Cleveland, 1973.
[35] Seybold, P. G.; Gouterman, M. *J. Mol. Spectrosc.* **1969**, *31*, 1.
[36] Quimby, D. J.; Longo, F. R. *J. Am. Chem. Soc.* **1975**, *97*, 5111.
[37] Laurence, C.; Nicolet, P.; Dalati, M. T.; Abboud, J.-L. M.; Notario, R. *J. Phys. Chem.* **1994**, *98*, 5807.
[38] Gouterman, M. *J. Mol. Spectrosc.* **1961**, *6*, 138.
[39] Segura, J. L.; Gómez, R.; Martín, N.; Luo, C. P.; Swartz, A.; Guldi, D. M. *Chem. Commun.* **2001**, 707.
[40] Luo, C.; Guldi, D. M.; Imahori, H.; Tamaki, K.; Sakata, Y. *J. Am. Chem. Soc.* **2000**, *122*, 6535.
[41] Armaroli, N.; Accorsi, G.; Gisselbrecht, J.; Gross, M.; Krasnikov, V.; Tsamouras, D.; Hadziioannou, G.; Gómez-Escalonilla, M. J.; Langa, F.; Eckerte, J.; Nierengarten, J. *J. Mater. Chem.* **2002**, *12*, 2077.
[42] Hsiao, J.-S.; Krueger, B. P.; Wagner, R. W.; Johnson, T. E.; Delaney, J. K.; Mauzerall, D. C.; Fleming, G. R.; Lindsey, J. S.; Bocian, D. F.; Donohoe, R. J. *J. Am. Chem. Soc.* **1996**, *118*, 11181.
[43] Trieflinger, C.; Röhr, H.; Rurack, K.; Daub, J. *Angew. Chem., Int. Ed. Engl.* **2005**, *44*, 6943.
[44] Kuciauskas, D.; Lin, S.; Seely, G. R.; Moore, A. L.; Moore, T. A.; Gust, D.; Drovetskaya, T.; Reed, C. A.; Boyd, P. D. W. *J. Phys. Chem.* **1996**, *100*, 15926.
[45] Alder, A. D.; Longo, F. R.; Finarelli, J. D.; Goldmacher, J.; Assour, J.; Korsakoff, L. *J. Org. Chem.* **1967**, *32*, 476.
[46] Fery-Forgues, S.; Bris, M. T. L.; Guette, J. P.; Valeur, B. *J. Phys. Chem.* **1988**, *92*, 6233.